NEOPLASIA
www.neoplasia.com

Volume 13 Number 5 May 2011 pp. 483–491 483

Metformin Suppresses Ovarian Cancer Growth and Metastasis with Enhancement of Cisplatin Cytotoxicity *In Vivo*[1,2]

Ramandeep Rattan, Rondell P. Graham, Jacie L. Maguire, Shailendra Giri and Viji Shridhar

Department of Experimental Pathology, Mayo Clinic College of Medicine, Mayo Clinic, Rochester, MN, USA

Abstract

Ovarian cancer is the most lethal gynecologic cancer in women. Its high mortality rate (68%) reflects the fact that 75% of patients have extensive (>stage III) disease at diagnosis and also the limited efficacy of currently available therapies. Consequently, there is clearly a great need to develop improved upfront and salvage therapies for ovarian cancer. Here, we investigated the efficacy of metformin alone and in combination with cisplatin *in vivo*. A2780 ovarian cancer cells were injected intraperitoneally in nude mice; A2780-induced tumors in nude mice, when treated with metformin in drinking water, resulted in a significant reduction of tumor growth, accompanied by inhibition of tumor cell proliferation (as assessed by immunohistochemical staining of Ki-67, Cyclin D1) as well as decreased live tumor size and mitotic cell count. Metformin-induced activation of AMPK/mTOR pathway was accompanied by decreased microvessel density and vascular endothelial growth factor expression. More importantly, metformin treatment inhibited the growth of metastatic nodules in the lung and significantly potentiated cisplatin-induced cytotoxicity resulting in approximately 90% reduction in tumor growth compared with treatment by either of the drugs alone. Collectively, our data show for the first time that, in addition to inhibiting tumor cell proliferation, metformin treatment inhibits both angiogenesis and metastatic spread of ovarian cancer. Overall, our study provides a strong rationale for use of metformin in ovarian cancer treatment.

Neoplasia (2011) 13, 483–491

Introduction

Ovarian cancer is the fifth leading cause of cancer death in women and the most lethal gynecologic malignancy [1]. Most patients present with advanced disease, and despite surgical debulking followed by platinum-based chemotherapy for advanced stage disease, the average time of clinical remission is approximately 2 years and the 5-year survival rate is 45% [2]. These data clearly highlight the need to identify new molecular targets and agents that can be used in the treatment of women with ovarian cancer.

Metformin is an antidiabetic drug that, during the last decade, has gained significant attention as an anticancer drug. Recently, owing to extensive reports of its *in vitro* and *in vivo* antitumor activity, many clinical trials have been initiated worldwide [3]. In patients with diabetes, it has been found to inhibit gluconeogenesis in the liver by impairing oxidative phosphorylation and leading to an imbalance of the AMP/ATP ratio. Consequently, metformin reduces blood glucose and insulin levels. The increased AMP levels also lead to the activation of LKB1-AMPK pathway. In cancer cells, AMPK activation by metformin and other activators results in inhibition of the mTOR pathway and modulates the expression of p21, p27, and cyclin D1, which inhibit proliferation. Although, initially it was believed that metformin's anticancer activity was through activation of AMPK-LKB1, recent data indicate it could also be independent of AMPK activation [4]. Consistent with these reports, our previous study in ovarian cancer cells indicated that the effect of metformin was partially dependent on AMPK but required LKB1 [5]. Although the precise mechanism for this phenomenon is currently not known, it is important to realize that metformin-mediated activation of LKB1 could also result in the

Address all correspondence to: Viji Shridhar, PhD, Department of Laboratory Medicine and Experimental Pathology, Mayo Clinic Cancer Center, Rochester, MN 55905.
E-mail: shridhar.vijayalakshmi@mayo.edu

[1]This work was supported by Fred C. and Katherine B. Andersen Foundation grant to V.S.

[2]This article refers to supplementary materials, which are designated by Figures W1 to W5 and are available online at www.neoplasia.com.

Received 14 January 2011; Revised 7 February 2011; Accepted 8 February 2011

DOI 10.1593/neo.11148

activation of other AMPK-related kinases. However, we cannot rule out the possibility that metformin, as a drug, may also be modulating other yet unidentified pathways.

In this study, we provide preliminary evidence that the action of metformin *in vivo* is multifaceted involving known biosynthetic pathways such as proliferation and protein biosynthesis and novel pathways such as modulation of angiogenesis and metastasis.

Materials and Methods

Reagents and Antibodies

A2780 cell lines were a kind gift of Dr Tom Hamilton (Fox Chase Cancer Center) and were grown in RPMI medium. Metformin (RIOMET 500 mg/5 ml) used for animals was purchased from Ranbaxy Laboratories (Princeton, NJ). Antibodies to phospho-ACC (cat. no. 3661, used at 1:100) and phospho-mTOR (cat. no. 2976, used at 1:50) were from Cell Signaling Technology (Denver, MA). Cyclin D1 (cat. no. sc753, used at 1:50) and CD31 (PECAM) (cat. no. sc31045, used at 1:100) were from Santa Cruz Biotechnology (Santa Cruz, CA); Ki-67 (cat. no. M7240, used at 1:100) was from Dako (Glostrup, Denmark), and vascular endothelial growth factor (VEGF; cat. no. ab3109, used at 1:50 for immunohistochemistry and 1:1000 for Western blot) antibody was purchased from Abcam (Cambridge, MA).

Animals

All animal experiments were done according to an Institutional Animal Care and Use Committee–approved protocol. Institutional guidelines for the proper and humane use of animals in research were followed. The facility has been approved by Association for Assessment and Accreditation of Laboratory Animal Care. Female nude mice were used between the ages of 6 and 7 weeks and purchased from the National Cancer Institute. Before injecting into animals, the cells were washed twice, counted, and resuspended in PBS at 2×10^6/100 μl. A2780 cells (2×10^6 suspended in 100 μl of PBS) were inoculated into the intraperitoneal cavity of mice (day 0). Treatment with metformin was started 7 days after inoculation of the cells. Metformin was dissolved in 200 ml of drinking water to attain the dosages of 100 and 200 mg/kg body weight. The water was changed daily and measured for water intake. Metformin treatment was continued for the next 3 weeks until the mice were killed at 4 weeks. The mice were monitored daily for any discomfort and weighed every third day to check for tumor growth. For combination studies, cisplatin treatment (4 mg/kg body weight) by intraperitoneal injections was given on days 7, 14, and 21 along with metformin treatment as described above (day 0 was taken as the day of inoculation of cells).

The main purpose of giving metformin in water was to maintain a constant level of metformin and sustained activation of AMPK in mouse as opposed to that achieved by a single dose, which gets cleared rapidly from the system. In patients, metformin is now preferably given in an extended release form, which can maintain the effect of metformin for a long duration and is therefore more effective. The XR tablet cannot be administered to animals because breaking or grinding the tablet compromises its slow-release ability (our experience and manufacturer's recommendation).

A recent well-established method to translate the dose of drugs used from one animal species to another has been published by Reagan-Shaw et al. [6] and also found at the National Cancer Institute Web site (http://dtp.nci.nih.gov). According to the formula, human equivalent dose (mg/kg) = animal dose (mg/kg) × animal K_m/human K_m, where species and K_m values are based on body surface area (K_m for adult human [60 kg] is 37 and mouse [20 g] is 3). On the basis of this formula, the human equivalent dose of 100 mg in mouse is 480 mg/average size person of 60 kg, which is five times lower than the maximum safe dose of 2550 mg/d recommended in the Physician's Desk Reference.

Cytotoxicity Assays

Blood was collected in heparin-coated tubes just before mice were killed. Plasma isolated from blood of 6 mice from each group was subjected to analysis of a panel of hepatic function tests (aspartate aminotransferase [AST], alanine aminotransferase [ALT], albumin), kidney function tests (creatinine, urea, albumin), and glucose. All assays were performed using kits from Bioassay Systems (Hayward, CA). All assays were performed according to the manufacturer's instructions.

Immunohistochemistry

The tumors excised from mice were fixed in 10% paraformaldehyde for 48 hours and paraffin-embedded. Four-micrometer-thick consecutive sections were cut and processed for immunohistochemistry for pACC (cat. no. 3661, used at 1:100), cyclin D1 (cat. no. sc753, used at 1:50), pmTOR (cat. no. 2976, used at 1:50), VEGF (cat. no. ab3109, used at 1:50), CD31 (cat. no. sc31045, used at 1:100), and Ki-67 (cat. no. M7240, used at 1:100). Solutions obtained from Dako Cytomation were used for performing immunostaining. In brief, tissue sections were deparaffinized, unmasked, blocked with avidin-biotin, and incubated with primary antibody overnight. Next day, the reaction was detected by using chromogen according to the manufacturer's instruction (Dako). The positive cells stained brown. The slides were examined under a light microscope, and representative pictograms were taken from a minimum of five or six different slides of each group. For CD31 staining, fluorescein isothiocyanate–labeled secondary antibody was used and visualized using fluorescent microscope in six sections per group.

Mitotic Count

The mitotic count was recorded on hematoxylin and eosin (H&E)–stained sections using the Olympus BX-41 light microscope (Center Valley, PA) at high-power field (HPF; ×400). Cells undergoing mitosis were counted in the tumors, in the most active area ("hot spots") in a minimum of five consecutive HPFs. The average number of cells undergoing mitosis per HPF was enumerated.

Live Tumor Measurements

The maximum diameter of viable tumor was calculated by summing the largest unidimensional diameter of each fragment of tumor using the Olympus BX-41 microscope and a micrometer. Similarly, necrotic areas were measured, and the composite live tumor size was calculated from each slide.

Western Blot

A small part of excised xenografts from four mice of each group was washed with PBS and immediately placed in 500 μl of protein lysis buffer (50 mM Tris-HCl, pH 7.5, 250 mM NaCl, 5 mM EDTA, 50 mM NaF, and 0.5% Nonidet P-40; containing a protease inhibitor cocktail [Sigma, St Louis, MO]). The tissue was homogenized, kept on ice for 30 minutes, and centrifuged at 10,000*g* for 10 minutes. Supernatant was separated, and protein concentration was estimated by the Bradford method (BioRad, Hercules, CA). Immunoblot analysis with VEGF antibody (1:100) was performed as previously described [5].

Statistical Analysis

Data were statistically analyzed using two-tailed Student *t*-test (Prism, La Jolla, CA) or the Student-Newman-Keuls test (GraphPad Software, La Jolla, CA). All animal experiments were performed at least twice with the minimum number of animals per group being six.

Results

Metformin Inhibits Ovarian Tumor Growth In Vivo

To determine whether metformin could curtail tumor growth *in vivo*, we injected A2780 cells intraperitoneally (IP) in nude mice (n = 11). On day 7, metformin (100 and 200 mg/kg body weight) was introduced in water as described in the Materials and Methods section. Addition of metformin to water did not affect water intake by mice (data not shown). At the end of 4 weeks, mice were killed and tumors were excised. Figure 1*A* (*top panel*) shows a representative photograph of the vivisected mouse showing tumors from different groups. Consistent with our previous *in vitro* report that metformin treatment of ovarian cancer cells leads to reduced proliferation, A2780 xenografts treated with metformin at two different concentrations had much reduced tumor burden compared with untreated mice (Figure 1*A*, *top* and *middle panels*). As previously reported by Shaw et al. [7], IP injected A2780 cells formed mainly solid tumors and presented with ovary-specific metastases (Figure 1*A*, *bottom panel*). The ovary-associated tumor mass in the metformin-treated mice was significantly smaller than that in the untreated mice. The mean weights of the excised tumors were approximately 50% and 60% less in mice treated with metformin

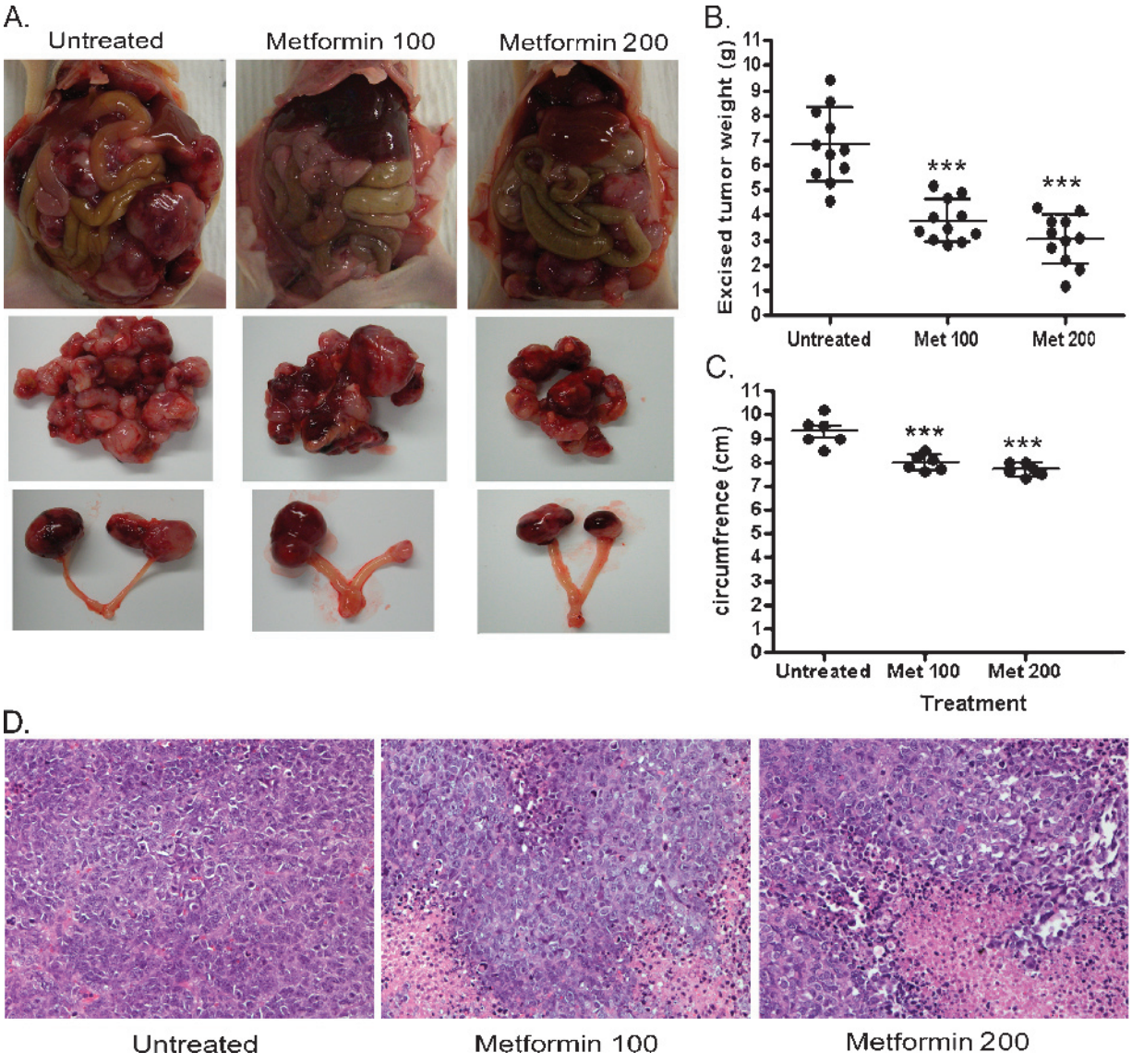

Figure 1. Metformin inhibits ovarian tumor growth *in vivo*. (A) Gross morphology of representative vivisected mouse showing A2780 tumors (top panel), excised tumor (middle panel), and tumors associated with ovary (lower panel) at 4 weeks from each group (n = 11). (B) Graph showing the excised tumor weight from each of each group (n = 11) with cumulative mean; untreated, Met 100 (metformin 100 mg/kg body weight), Met 200 (metformin 200 mg/kg body weight). ***P < .001, treated compared with the untreated group. (C) Cumulative abdominal circumference from untreated, metformin 100 mg/kg body weight (Met 100) and metformin 200 mg/kg body weight (Met 200) (n = 11) at 4 weeks. ***P < .001, treated compared with the untreated group. (D) Representative photomicrographs of H&E (×200)–stained ovarian cancer xenografts from each group.

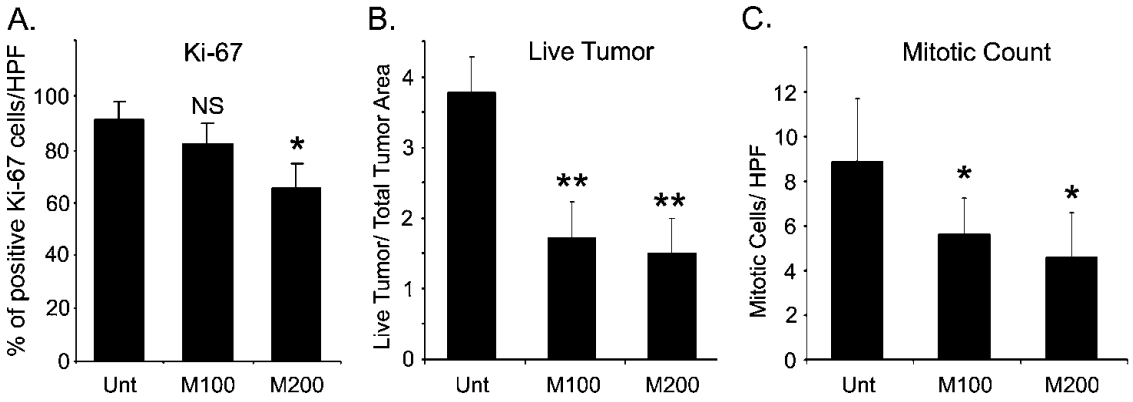

Figure 2. Metformin inhibits proliferation of ovarian tumors *in vivo*. (A) Count of positive Ki-67–stained cells from five HPFs in each of three different tumors from each group (×400) expressed as percentage. (B) Measurement of viable tumor size as described in Materials and Methods. (C) Mitotic counts per HPF (×400) counted from five fields of three different tumors from each group. $^{**}P < .05$, $^{*}P < .01$, treated groups compared with untreated.

100 (3.06 ± 0.06 g) and 200 mg/kg body weight (2.86 ± 0.52 g), respectively, compared with untreated mice (6.72 ± 0.52 g; Figure 1*B*). Also, the abdominal circumference, which is indicative of the tumor burden being carried in the peritoneum, was significantly less in the treated mice compared with untreated mice (Figure 1*C*). Representative portions of the excised tumors were paraffin-fixed and processed for histologic examination. On review of the H&E–stained slides, the morphology of the excised masses (Figure 1*D*) was consistent with that of epithelial ovarian carcinoma.

Although metformin has a strong safety record in human consumption, we determined whether metformin treatment results in any cytotoxicity when given to mice with ovarian tumors. Plasma isolated from blood of six mice from the untreated group and from those treated with 200 mg/kg was subjected to analysis of a panel of hepatic function (AST, ALT, and albumin) and kidney function tests (creatinine, urea [serum urea nitrogen], albumin). There was no significant difference between the untreated and metformin-treated mice, and all values were well within the normal limits (Figure W1). We also determined the glucose levels because metformin is known to lower glucose levels in patients with diabetes. There was no significant difference between the glucose levels of untreated and metformin-treated mice, indicating that metformin does not affect the glucose levels in nondiabetic conditions (Figure W1).

These data thus reflect the efficacy of metformin in inhibiting the growth of human ovarian cancer cells *in vivo*.

Metformin Inhibits Proliferation of Ovarian Tumors In Vivo

To investigate if metformin acts by inhibiting proliferation as previously reported by us and others *in vitro*, we performed immunohistochemistry for Ki-67. Ki-67 staining did not show any significant difference in the intensity of the staining between treated and untreated mice (Figure W2*A*; ×100). To obtain a more clear picture, we performed a count of Ki-67–positive cells in five HPFs in each of three different tumors from treated and untreated mice (Figure 2*A*). The counts were expressed as percentage of positive cells per field. Although, metformin at the 100-mg/kg treatment did not show a significant difference, xenografts treated with metformin 200 mg/kg showed significantly less Ki-67–positive cells, indicating that less percentage of cells were proliferating under metformin treatment. This maybe attributed to our previously shown observation that metformin treatment *in vitro* results in G_1 cell cycle arrest [5], which may also affect the Ki-67 index because Ki-67 indicates that the cell has entered the cell cycle but does not provide the information if the cells passes through G_1/S or G_2/M phases. To further assess the viability of the tumor, necrotic and viable tumor size was determined from H&E–stained sections (Figure W2*B*, circled regions for necrotic areas of the tumor; ×20). The ratio of live tumor size to total tumor size was calculated based on the largest unidimensional diameter as described in Materials and Methods. As shown in Figure 2*B*, xenografts derived from metformin-treated mice had significantly less viable tumor sizes and more necrotic regions compared with xenografts derived from untreated mice. Consistent with this observation, mitotic count measured as described in the Materials and Methods section was higher in the xenografts derived from untreated mice compared with mice treated with metformin (Figure 2*C*). Collectively, these data demonstrate that metformin treatment inhibits proliferation *in vivo* resulting in reduced tumor size consistent with the *in vitro* studies.

Metformin Inhibits Metastasis and Angiogenesis in Ovarian Tumors In Vivo

To determine whether metformin treatment had any effect on metastasis, we did H&E staining of various organs. Although tumor was visible on liver, spleen, and kidney in untreated mice, we did not see any invasion of these tumors into these organs (data not shown). However, significant pulmonary metastasis was seen in the lungs of untreated mice but not in metformin-treated mice (Figure 3*A*). Enumeration of the number of metastatic nodules in the lung sections of five different mice from each group also revealed presence of significantly less nodules in treated *versus* untreated mice (Figure 3*Di*). In addition, because new blood vessel formation is a requirement for tumors to grow and metastasize, we evaluated the microvasculature density in the xenografts. Anti-CD31 staining showed reduced microvessel density in metformin-treated tumors (Figure 3*B*, ×200) compared with untreated mice, indicative of inhibition of angiogenesis. Furthermore, quantification of positively stained vessels done in five HPFs (×400) of three sections each also confirmed reduced angiogenesis (Figure 3*Dii*). In addition to the reduced microvessel density, there was significantly less staining and expression of VEGF (Figure 3*C*, ×200; Figure 3*Dii*) in xenografts of metformin-treated mice compared with untreated mice, further substantiating inhibition

of angiogenesis in metformin-treated mice. Collectively, these data suggest the potential of metformin in attenuating metastasis and angiogenesis, two essential processes required for tumor growth and sustenance.

Metformin Induces AMPK in Ovarian Tumors In Vivo

The main mechanism of action of metformin is activation of AMPK and modulation of its downstream effectors. To assess if metformin treatment results in activation of AMPK, we stained the tumor sections for pACC, the direct downstream target of AMPK. The tumors showed some basal expression of pACC, which was significantly increased in a dose-dependent manner (100 and 200 mg/kg body weight) with metformin treatment (Figure 4*A*; ×200). This was also confirmed by scoring of percentage positive cells per five HPF (400×) from five different sections from each animal group (Figure 4*D*, *first panel*). This suggests

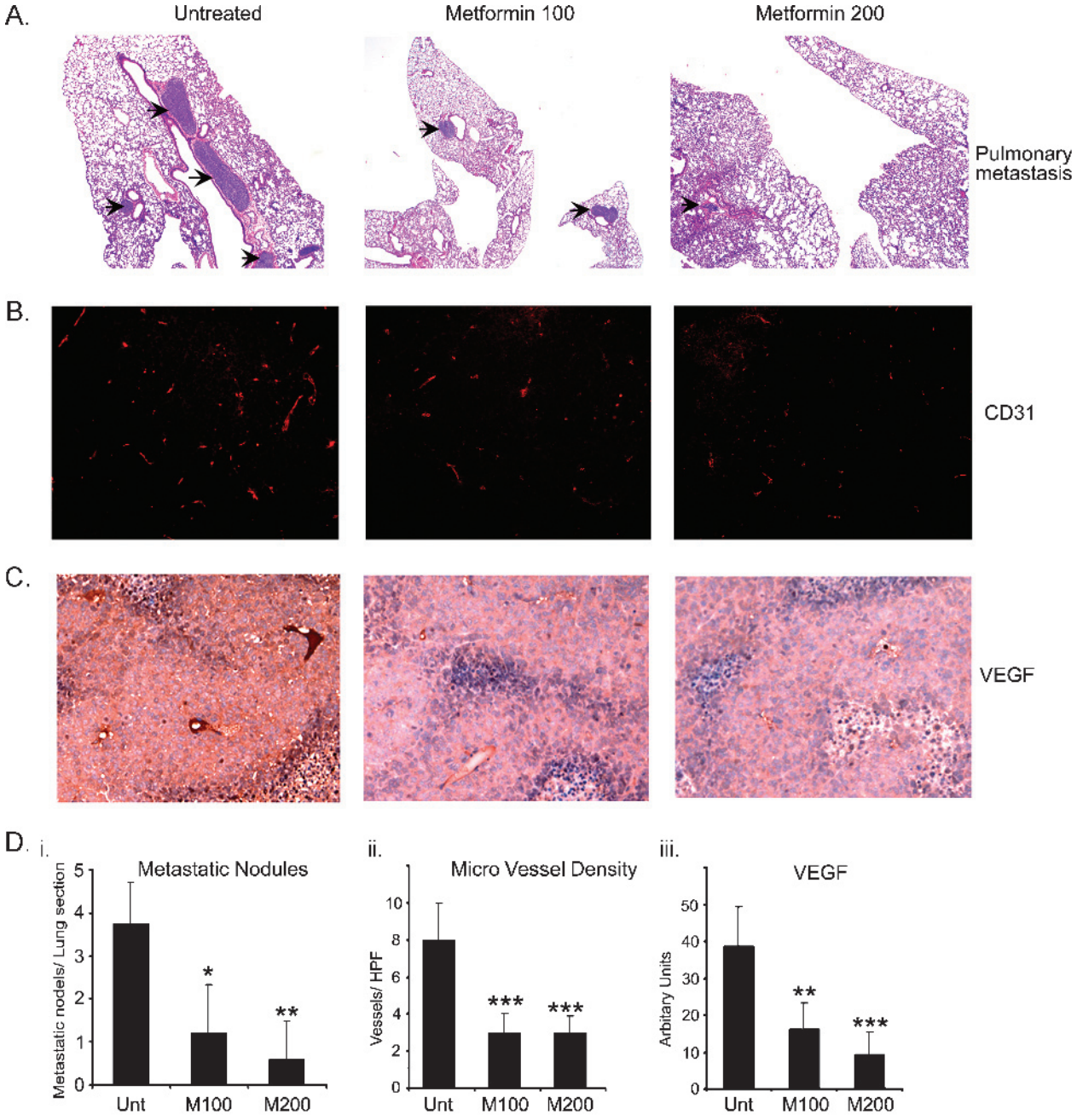

Figure 3. Metformin inhibits metastasis and angiogenesis in ovarian tumors *in vivo*. (A) Representative photomicrographs of H&E (×100)–stained lung tissues exhibiting metastasized ovarian cancer from each group. The metastatic nodules are pointed out with arrows. Lung sections from five different mice were examined. (B) Representative staining of CD31 of blood microvessels (×200) of A2780 xenografts in mice at 4 weeks. (C) Representative staining of VEGF (×400) in A2780 xenografts in mice at 4 weeks performed in five sections from each group. (D) Di: Enumeration of average number of pulmonary metastatic nodules from five H&E–stained lung sections. Dii: Count of average microvessels per HPF (×400) from five fields of three different tumor sections. Diii: Expression of VEGF was determined by Western blot from protein of tumor tissue of four individual mice per group. Graph represents the densitometric average of each group. ***$P < .001$, **$P < .05$, *$P < .01$, treated groups compared with the untreated group.

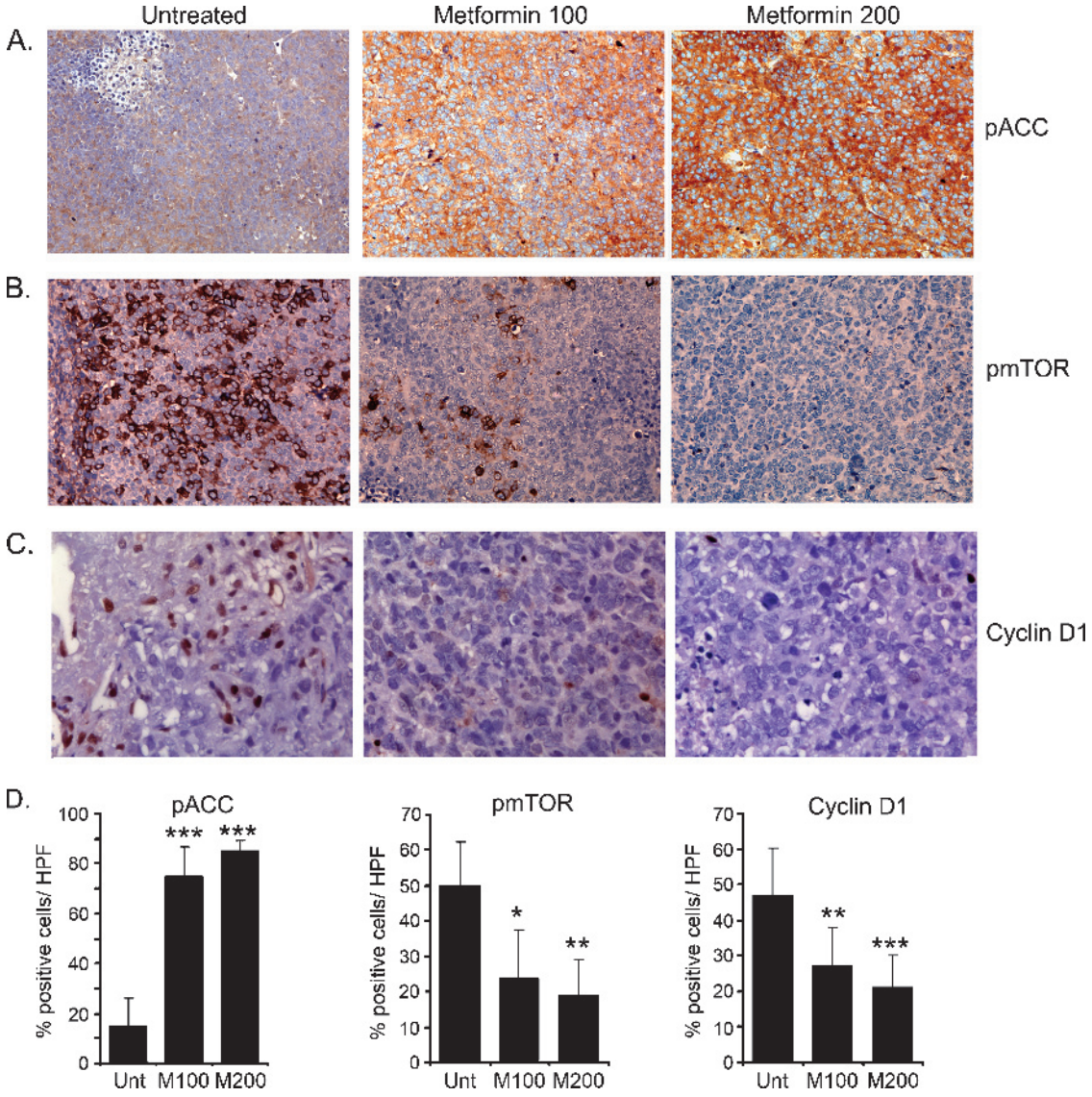

Figure 4. Metformin induces AMPK in ovarian tumors *in vivo* and its downstream effectors. Representative staining of pACC (A, ×200), p-mTOR (B, ×200, and cyclin D1 (C, ×400) seen in tumor sections from each group. Five slides from each group were stained. (D) Graphical representation of percentage of positive cells counted from five HPFs (400×) per section of five different slides from each animal group. M100 indicates metformin 100 mg/kg; M200, metformin 200 mg/kg; Unt, untreated. ***$P < .001$, **$P < .05$, *$P < .01$, treated groups compared with the untreated group.

that metformin is taken up by the tumors when given orally. To further confirm that AMPK activation also leads to activation/inhibition of its downstream targets, we stained for markers, which we have previously shown *in vitro* to be modulated by metformin [5]. Metformin treatment was able to inhibit the expression of p-mTOR (Figure 4*B*; ×200) and cyclin D1 (Figure 4*C*; ×400). This was also confirmed by the scoring of percentage positive cells per five HPF (400×) from five different sections from each animal group (Figure 4*D*, *second and third panels*). These data strongly suggest that metformin treatment results in AMPK activation in tumor tissues and modulates cell cycle and protein synthesis to restrain tumor growth. Our repeated attempts using individual mouse tumors ($n = 6$) to determine the expression of the same protein markers by immunoblot analysis gave inconsistent results (data not shown). This may be due to several reasons such as tumor heterogeneity and/or the areas of the tumors used for protein extraction. This is particularly important because we used small amounts of tissue for lysate preparation without the knowledge of whether the tissues used contained regions of necrosis.

Metformin Potentiates Cisplatin-Induced Cytotoxicity in Inhibiting Tumor Growth

Metformin and/or cisplatin treatment of A2780 and its cisplatin-resistant isogenic C200 cells *in vitro* significantly inhibited colony-forming abilities and resulted in reduced colony formation (Figure W3). Therefore, after the generation of A2780 xenografts, the mice were treated with two different doses of metformin (100 and 200 mg/kg body weight). Weekly IP injections of cisplatin on days 7, 14, and 21 along with continuous metformin therapy were very effective in inhibiting the tumor growth. The combination of cisplatin (4 mg) with metformin 100 mg/kg body weight (2.08 ± 0.18 g; Figure 5*A*) significantly reduced tumor growth compared with metformin 100 mg/kg body weight (3.54 ± 0.35 g) or cisplatin treatment alone (3.15 ± 0.34 g) or

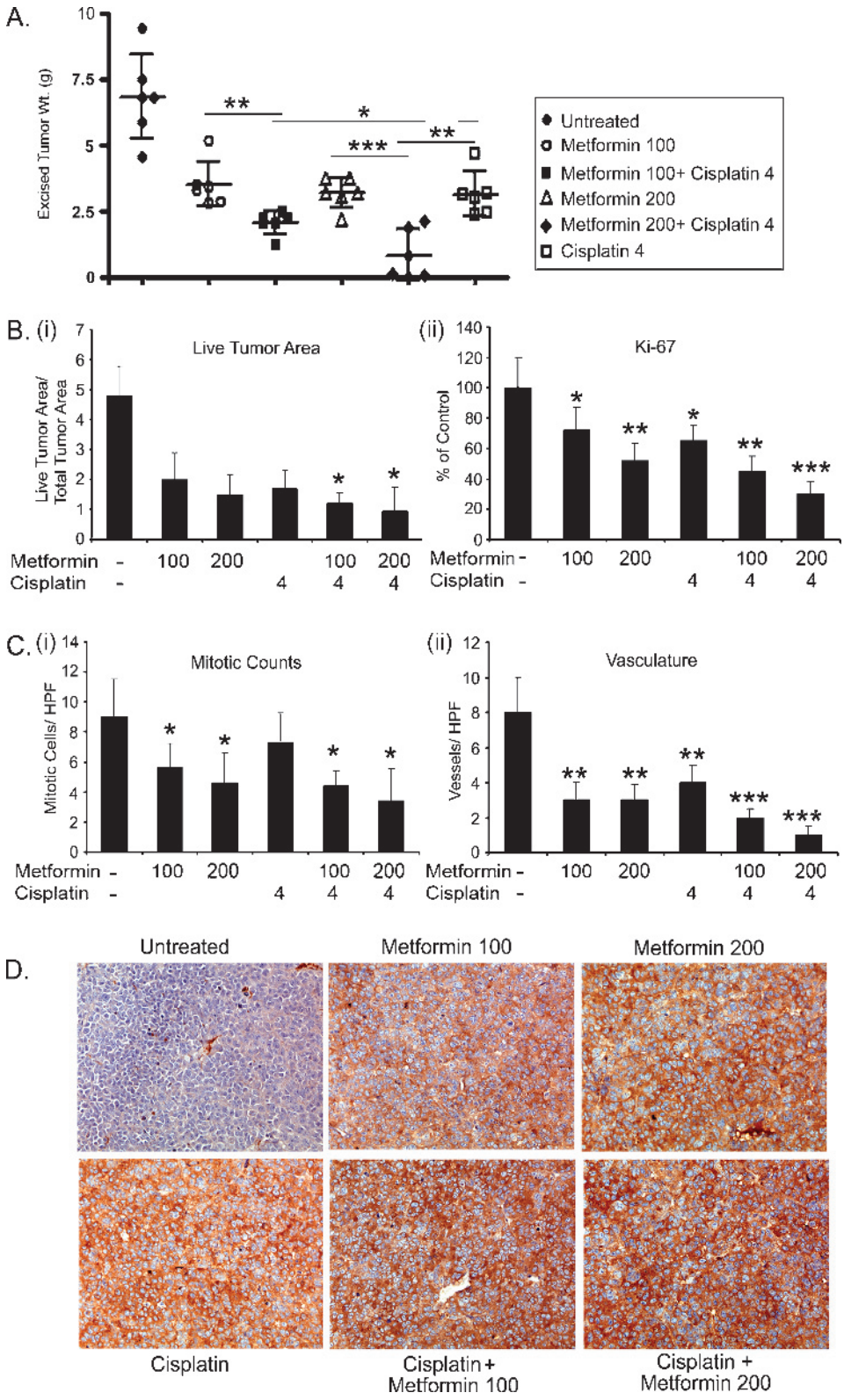

Figure 5. Metformin and cisplatin effectively combine to inhibit ovarian tumor growth. (A) Cumulative excised tumor weight from individual mice bearing A2780 xenografts at 4 weeks ($n = 6$) with metformin 100 and 200 mg/kg body weight in combination with cisplatin (4 mg). ***$P < .001$, **$P < .05$, *$P < .01$, metformin and cisplatin combination–treated groups compared with single-drug–treated group. (B) Bi: Graphical representation of viable tumor size measured from four different tumors as described before. *$P < .01$, combination compared with metformin and cisplatin treatment alone. Bii: Positive Ki-67 cells measured from four different tumors as described before and is represented as percentage of control. ***$P < .001$, **$P < .05$, *$P < .01$, treated groups compared with the untreated group. (C) Ci: Mitotic counts per HPF from six fields of three different tumors from each group. *$P < .01$, treated groups compared with the untreated group. Cii: Vessel counts per HPF (×400) from six HPFs of three tumors from each group. ***$P < .001$, **$P < .05$, treated groups compared with the untreated group. (D) Representative (×200) staining showing pACC indicating AMPK activation in tumor tissues excised from mice at 4 weeks.

untreated mice (6.9 ± 0.66 g). The effect of cisplatin and metformin at 200 mg/kg body weight (0.84 ± 0.39 g) was even more pronounced compared with metformin 200 mg/kg body weight alone (2.65 ± 0.23 g; Figure 5*A*). Tumor volume was reduced by ~90% in most of the mice, whereas three of six mice had no visible tumors. A representation of the H&E micrographs is shown in Figure W4.

Measurement of live tumor size was also further reduced in metformin and cisplatin combination treatments (Figure 5*Bi*), along with significantly less Ki-67 index (Figure 5*Bii*). Similarly, mitotic activity was less in cases of metformin and cisplatin–treated mice when compared with cisplatin-alone–treated mice (Figure 5*Ci*). Interestingly, the most significant differences were seen in the microvessel count as ascertained by CD31 staining of the xenografted sections, where the combination of metformin and cisplatin–treated mice had significantly less vascular density than either metformin or cisplatin alone (Figure 5*Cii*). Cisplatin treatment on its own strongly induced AMPK activity as seen by pACC staining (Figure 5*D*) and was further enhanced with metformin combinations, indicating that cisplatin can also activate the AMPK pathway. Collectively, these results suggest that combining metformin with cisplatin treatment is very effective, leading to decreased tumor size and also angiogenesis.

Discussion

This is the first report demonstrating the *in vivo* potential of metformin and its enhanced effectiveness with cisplatin in ovarian cancer in reducing tumor burden, angiogenesis, and metastatic potential. In this study, we demonstrate that metformin treatment of IP-induced A2780 xenografts resulted in (1) reduced tumor size in nude mice, (2) less metastatic nodules in lungs compared with untreated mice, (3) decreased proliferation as determined by low Ki-67 index and mitotic count and decreased cyclin D1 expression, (4) diminished angiogenesis as determined by VEGF inhibition and from vascular density on CD31 staining, (5) increased activity of AMPK as observed by pACC levels and decreased pmTOR expression, and (6) potentiated cisplatin-induced cytotoxicity compared with either agent alone. Overall, our data strongly support metformin as an anticancer agent for ovarian cancer and suggest that combining metformin with cisplatin can increase the efficacy of cisplatin-induced cytotoxicity.

Several *in vivo*–based studies have demonstrated that metformin can effectively inhibit growth of colon, pancreatic, mammary adenocarcinomas, and lung carcinoma cells in AMPK-dependent and -independent mechanisms [4]. Schneider et al. [8] showed that metformin treatment *in vivo* resulted in the inhibition of pancreatic cancer in hamsters fed a high-fat diet. Similarly, other studies have shown that metformin specially inhibits the growth of tumors induced on a high-fat diet [9]. Studies in breast cancer showed that metformin treatment significantly decreased the tumor burden and accumulation of mammary adenocarcinomas accompanied by increase in the life span of HER-2/*neu* transgenic mice [10]. In these initial reports, the authors speculated that the *in vivo* effects of metformin might be due to reducing insulin levels and mimicking a calorie restriction state. Additional reports directly implicated activation of AMPK by metformin. Metformin also reduced the size of intestinal polyps while not affecting the number in ApcMin/+ mice, which was attributed to AMPK-mediated inhibition of mTOR-S6K protein synthesis pathway [11]. In prostate cancers, metformin treatment resulted in decreased proliferation by cyclin D1 [12].

Consistent with the aforementioned studies, we have shown that metformin is effective in inhibiting *in vivo* tumor burden of ovarian xenografts, alone and in combination with cisplatin. We have also analyzed the biomarkers of these phenotypic effects, that is, activation of AMPK (by pACC) and inhibition in activation of mTOR and cyclin D1 expression. One of our novel observations is that we show for the first time that metformin treatment alone resulted in decreased blood microvessel density (CD31 staining) and reduced VEGF levels in the ovarian cancer xenografts, implicating an important and previously unidentified effect of metformin in inhibiting angiogenesis *in vivo*. This is in contrast to studies that have shown that AMPK activation by various means induces VEGF expression and or angiogenesis [13–15]. AMPK activation in DU145 cells under glucose deprivation resulted in increased levels of VEGF mRNA stability via the JNK-ROS pathway, independent of HIF-1 and/or LKB1 activation. Metformin-induced inhibition of angiogenic phenotype in our study is in contrast to the above-mentioned reports. This could be attributed to differences in the experimental conditions such as the *in vivo* setting in our study and the absence of external nutritional stress to activate AMPK. In addition, in the *in vitro*–based studies cited above, activation of AMPK was likely transient rather than sustained as in our *in vivo* studies due to continuous uptake of metformin in drinking water. In other non–cancer-related studies, HMEC cells exposed to serum from polycystic ovarian syndrome patients on metformin treatment resulted in decreased migration and invasion of these cells through inhibition of nuclear factor-κB, Erk1/2, and Erk 5, resulting in increased thrombospondin-1 expression, an antiangiogenic adipokine [16]. Phosphorylation of LKB1 at S307 (a site that is also phosphorylated after metformin treatment) leads to activation of AMPK and results in attenuation of angiogenesis. This suggests a link between activation of LKB1-AMPK pathway by metformin and diminished angiogenesis. Inhibition of inflammatory angiogenesis in a murine sponge model by metformin provides additional supporting data on the effect of metformin on endothelial cells [17]. Although the precise mechanism by which metformin attenuates angiogenic phenotype is currently not known, we do not rule out the possibility that this phenomenon may be complex, involving other pathways that are not regulated by AMPK, and may also be cell type dependent.

Another novel observation that we report is the inhibition of metastasis by metformin as demonstrated by significantly fewer and smaller metastatic nodules in the lungs of treated mice compared with control mice. Because activation of mTOR-S6K pathway is associated with the epithelial-mesenchymal transition phenotype, attenuation of metastasis seen in our study could be due to the inhibition of mTOR pathway by metformin. Additional studies are underway to determine the mechanistic basis of this novel observation. Whereas metformin has been shown to inhibit *in vitro* migration and invasion of human fibrosarcoma cells, metformin did not inhibit lung metastasis in an *in vivo* metastatic breast cancer model [18,19].

Very few reports are available citing effects of metformin and cisplatin combination. Whereas Gotlieb et al. [20] reported metformin to enhance cisplatin cytotoxicity in ovarian cancer cells *in vitro*, Harhaji-Trajkovic et al. [21] reported metformin to protect cells from cisplatin by inducing autophagy in glioma cells . Our data show a significant inhibition of ovarian cancer growth when both agents are given *in vitro* and *in vivo*. On the basis of the inhibition seen in colony formation assay with platinum-resistant C200 subline of A2780, we can speculate that metformin will also be able to limit the growth of platinum-resistant ovarian tumors. Additional experiments with more platinum-resistant ovarian cancer cell lines *in vitro* and *in vivo* will

help to answer this better. Cisplatin treatment also resulted in activation of AMPK as reported earlier [21]. Whether the enhanced antitumor effect of the combination is due to activation of AMPK by cisplatin or by augmentation of cytotoxicity by metformin remains to be determined.

What is currently unknown is whether metformin's antitumor effect is due to the direct effect on the growing tumor or due to its potential to alter host physiology or a combination of both of these effects. In our study, we found that metformin treatment increases AMPK activation in both the tumor tissue and also potently in the liver (Figure W5). Moreover, metformin has systemic, organism-wide effects by reducing glucose levels, reducing insulin and IGF signaling. We postulate that that the anticancer effect of metformin occurs both at the cellular and at the organismal levels simultaneously. The changes that occur in the tumor tissue are mainly at the cellular level leading to changes in the signaling events (cyclin D1, p21, mTOR). Concomitantly, there is modulation of the host AMPK activity, which redirects the host physiology (insulin, IGF, gluconeogenesis, lipid pathways, leptin, adiponectin) and mimics a state of caloric restriction. All of these host changes have been shown in preclinical studies to be associated with a better outcome in patients with cancer. Additional *in vivo* studies are needed to dissect these effects of metformin to gain a better understanding of its mechanism of action.

Along with the large number *in vitro* and *in vivo* studies detailing metformin's anticancer activities and the recent reports of its ability to target stem cells [22], there are also mounting retrospective data from population-based studies, mainly from diabetic populations, supporting its ability to reduce cancer risk and better outcome of different cancers [4]. On the basis of these studies, metformin is now being used in various clinical trails including in a neoadjuvant setting and in combination with other drugs [3].

Collectively, our data support the use of metformin as an anticancer drug alone or in combination with standard chemotherapeutic agents that suppress proliferation, protein synthesis, angiogenesis, and metastasis. Therefore, it provides a strong rationale for using metformin as a therapeutic drug in combination with cisplatin in the treatment of patients with ovarian cancer.

References

[1] Jemal A, Siegel R, Xu J, and Ward E (2010). Cancer statistics, 2010. *CA Cancer J Clin* **60**, 277–300.

[2] Aletti GD, Gallenberg MM, Cliby WA, Jatoi A, and Hartmann LC (2007). Current management strategies for ovarian cancer. *Mayo Clin Proc* **82**, 751–770.

[3] Gonzalez-Angulo AM and Meric-Bernstam F (2010). Metformin: a therapeutic opportunity in breast cancer. *Clin Cancer Res* **16**, 1695–1700.

[4] Ben Sahra I, Le Marchand-Brustel Y, Tanti JF, and Bost F (2010). Metformin in cancer therapy: a new perspective for an old antidiabetic drug? *Mol Cancer Ther* **9**, 1092–1099.

[5] Rattan R, Giri S, Hartmann L, and Shridhar V (2009). Metformin attenuates ovarian cancer cell growth in an AMP-kinase dispensable manner. *J Cell Mol Med* **15**, 166–178.

[6] Reagan-Shaw S, Nihal M, and Ahmad N (2008). Dose translation from animal to human studies revisited. *FASEB J* **22**, 659–661.

[7] Shaw TJ, Senterman MK, Dawson K, Crane CA, and Vanderhyden BC (2004). Characterization of intraperitoneal, orthotopic, and metastatic xenograft models of human ovarian cancer. *Mol Ther* **10**, 1032–1042.

[8] Schneider MB, Matsuzaki H, Haorah J, Ulrich A, Standop J, Ding XZ, Adrian TE, and Pour PM (2001). Prevention of pancreatic cancer induction in hamsters by metformin. *Gastroenterology* **120**, 1263–1270.

[9] Algire C, Amrein L, Zakikhani M, Panasci L, and Pollak M (2010). Metformin blocks the stimulative effect of a high-energy diet on colon carcinoma growth *in vivo* and is associated with reduced expression of fatty acid synthase. *Endocr Relat Cancer* **17**, 351–360.

[10] Anisimov VN, Berstein LM, Egormin PA, Piskunova TS, Popovich IG, Zabezhinski MA, Kovalenko IG, Poroshina TE, Semenchenko AV, Provinciali M, et al. (2005). Effect of metformin on life span and on the development of spontaneous mammary tumors in HER-2/*neu* transgenic mice. *Exp Gerontol* **40**, 685–693.

[11] Tomimoto A, Endo H, Sugiyama M, Fujisawa T, Hosono K, Takahashi H, Nakajima N, Nagashima Y, Wada K, Nakagama H, et al. (2008). Metformin suppresses intestinal polyp growth in ApcMin/+ mice. *Cancer Sci* **99**, 2136–2141.

[12] Ben Sahra I, Laurent K, Loubat A, Giorgetti-Peraldi S, Colosetti P, Auberger P, Tanti JF, Le Marchand-Brustel Y, and Bost F (2008). The antidiabetic drug metformin exerts an antitumoral effect *in vitro* and *in vivo* through a decrease of cyclin D1 level. *Oncogene* **27**, 3576–3586.

[13] Nagata D, Mogi M, and Walsh K (2003). AMP-activated protein kinase (AMPK) signaling in endothelial cells is essential for angiogenesis in response to hypoxic stress. *J Biol Chem* **278**, 31000–31006.

[14] Phoenix KN, Vumbaca F, and Claffey KP (2009). Therapeutic metformin/AMPK activation promotes the angiogenic phenotype in the ERα negative MDA-MB-435 breast cancer model. *Breast Cancer Res Treat* **113**, 101–111.

[15] Yun H, Lee M, Kim SS, and Ha J (2005). Glucose deprivation increases mRNA stability of vascular endothelial growth factor through activation of AMP-activated protein kinase in DU145 prostate carcinoma. *J Biol Chem* **280**, 9963–9972.

[16] Tan BK, Adya R, Chen J, Farhatullah S, Heutling D, Mitchell D, Lehnert H, and Randeva HS (2009). Metformin decreases angiogenesis via NF-κB and Erk1/2/Erk5 pathways by increasing the antiangiogenic thrombospondin-1. *Cardiovasc Res* **83**, 566–574.

[17] Xavier DO, Amaral LS, Gomes MA, Rocha MA, Campos PR, Cota BD, Tafuri LS, Paiva AM, Silva JH, Andrade SP, et al. (2010). Metformin inhibits inflammatory angiogenesis in a murine sponge model. *Biomed Pharmacother* **64**, 220–225.

[18] Hwang YP and Jeong HG (2010). Metformin blocks migration and invasion of tumour cells by inhibition of matrix metalloproteinase-9 activation through a calcium and protein kinase Cα–dependent pathway: phorbol-12-myristate-13-acetate–induced/extracellular signal–regulated kinase/activator protein-1. *Br J Pharmacol* **160**, 1195–1211.

[19] Phoenix KN, Vumbaca F, Fox MM, Evans R, and Claffey KP (2010). Dietary energy availability affects primary and metastatic breast cancer and metformin efficacy. *Breast Cancer Res Treat* **123**, 333–344.

[20] Gotlieb WH, Saumet J, Beauchamp M-C, Gu J, Lau S, Pollak MN, and Bruchim I (2008). *In vitro* metformin anti-neoplastic activity in epithelial ovarian cancer. *Gynecol Oncol* **110**, 246–250.

[21] Harhaji-Trajkovic L, Vilimanovich U, Kravic-Stevovic T, Bumbasirevic V, and Trajkovic V (2009). AMPK-mediated autophagy inhibits apoptosis in cisplatin-treated tumour cells. *J Cell Mol Med* **13**, 3644–3654.

[22] Hirsch HA, Iliopoulos D, Tsichlis PN, and Struhl K (2009). Metformin selectively targets cancer stem cells, and acts together with chemotherapy to block tumor growth and prolong remission. *Cancer Res* **69**, 7507–7511.

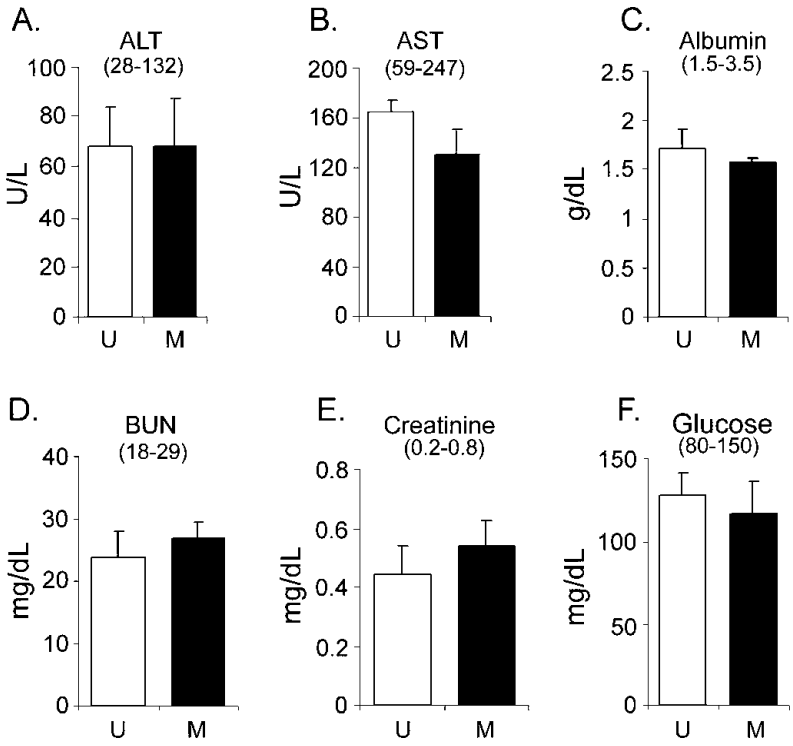

Figure W1. Cytotoxic profile in plasma from A2780 tumor-bearing mice with or without metformin treatment. Before sacrificing the mice at 4 weeks, blood was collected in heparin-coated tubes, and plasma was separated. Mouse plasma from untreated group (U) and metformin 200 mg/kg (M) were subjected to a panel of cytotoxic tests according to the manufacturer's instructions: (A) ALT, (B) AST, (C) albumin, (D) BUN (serum urea nitrogen), (E) creatinine, and (F) glucose.

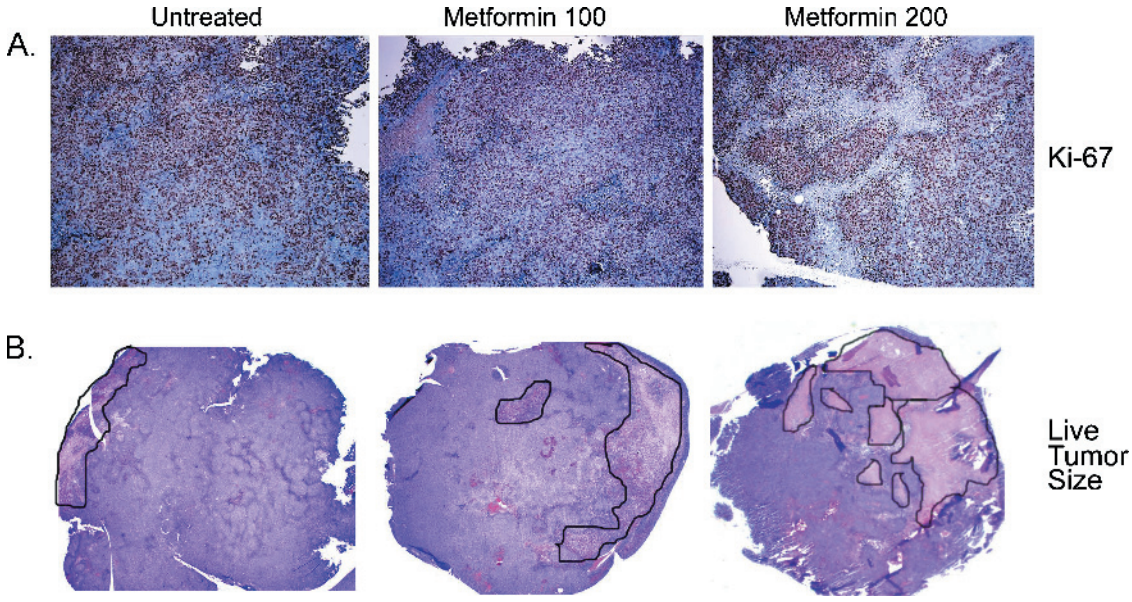

Figure W2. (A) Representative Ki-67 staining (×200) of excised A2780 tumors at 4 weeks. (B) Necrotic/dead areas were excluded, and viable tumor was measured and divided by the total tumor dimension from three H&E sections (×20). Representative pictures (×20) show encircled necrotic area excluded from viable tumor measurements.

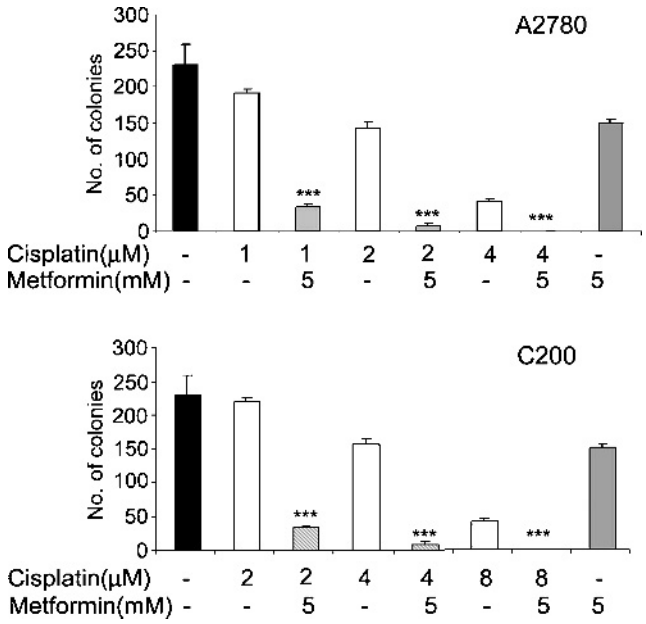

Figure W3. Metformin inhibits colony formation in A2780 and C200 cells. A total of 2000 cells/well (A2780, C200) in six-well plates were treated with indicated concentrations of cisplatin once. Metformin treatments were done every third day for 2 to 3 weeks until colonies were formed. The colonies were stained with MTT and counted. Data represent three separate experiments done in triplicates. ***$P < .001$, compared with untreated cells.

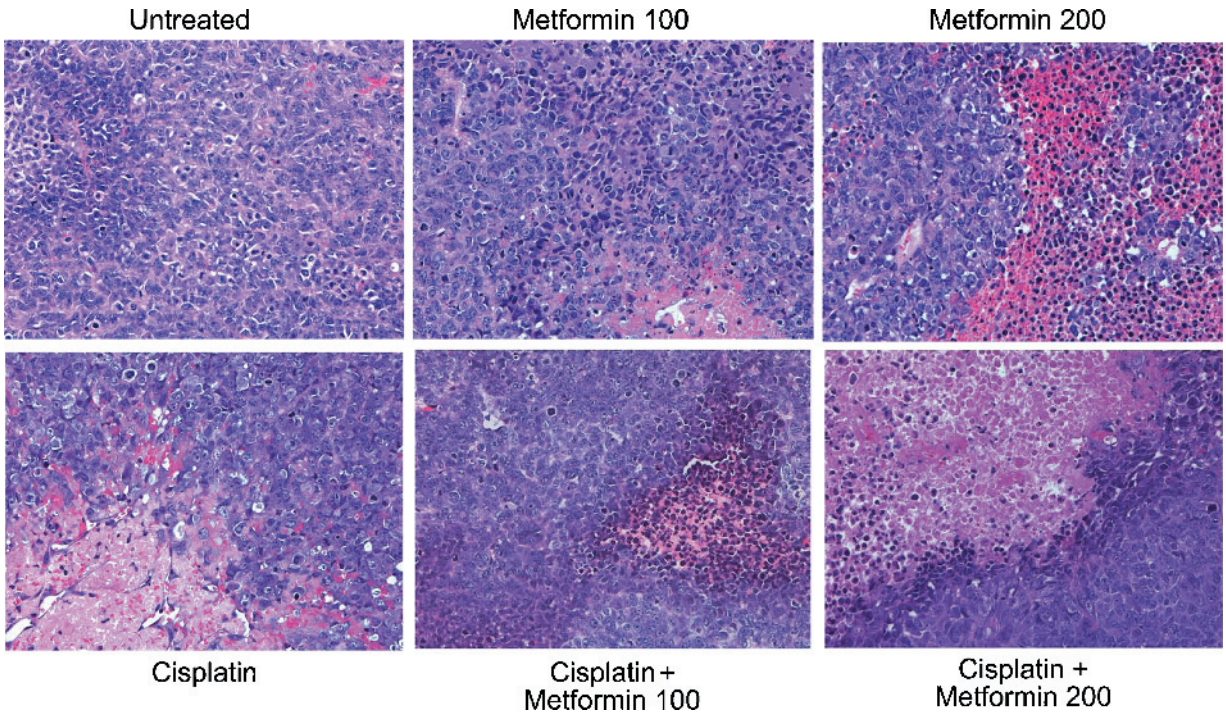

Figure W4. Representative H&E (×200) staining showing morphology of A2780 ovarian tumors in mice at 4 weeks.

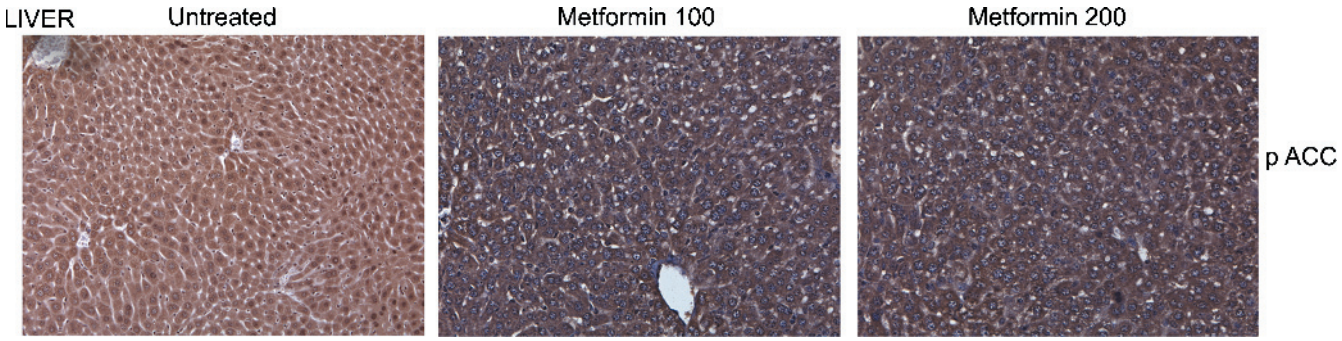

Figure W5. Representative (×200) staining showing pACC indicating AMPK activation in liver tissues excised from mice at 4 weeks.